

## INFLUENCE OF DEFECTS ON LIMIT LOADS AND INTEGRITY OF THE PIPELINE AT HYDROPOWER PLANT 'PIROT'

### UTICAJ OŠTEĆENJA NA NOSIVOST I INTEGRITET CEVOVODA HIDROELEKTRANE 'PIROT'

Originalni naučni rad / Original scientific paper  
UDK /UDC:

Rad primljen / Paper received: 29.11.2019

Adrese autora / Authors' addresses:

<sup>1</sup>) University of Belgrade, Faculty of Technology and Metallurgy, Belgrade, Serbia email: [bmedjo@tmf.bg.ac.rs](mailto:bmedjo@tmf.bg.ac.rs)

<sup>2</sup>) Institute for Materials Testing (IMS), Belgrade, Serbia

<sup>3</sup>) Euro-Mont-Ing, Belgrade, Serbia

#### Keywords

- pipeline
- integrity assessment
- finite element method
- FAD diagram

#### Abstract

Topic of this work is the integrity assessment of the pipeline section from hydropower plant Pirot. Crack-like defect size, maximum depth, is determined based on non-destructive evaluation - the largest crack depth is taken as the initial value for load carrying capacity estimation. Also, the crack dimensions (both length and depth) are varied. Limit pressure values are determined from 3D and 2D models of pipes with axial cracks on external surface. The influence of tensile loading on the load carrying capacity of the pipes with circumferential cracks is also examined. Integrity of pipes with both types of defects (axial and circumferential) is assessed through application of FAD diagrams.

#### INTRODUCTION

Different defects that originate from production, assembly/joining or exploitation of pipeline elements, can have a significant influence on the load carrying capacity and work safety of pressurised systems. Since the reliability and safety of pressurised equipment elements is very important for efficient production, there are many studies that deal with the influence of defects such as cracks, volumetric defects (e.g. caused by corrosion, erosion, cavitation), welding defects, etc., on the resistance to failure, /1-9/.

The pipeline considered in this work is in exploitation in the hydropower plant 'Pirot' in Serbia. Integrity assessment is performed by using the finite element method, considering both fracture initiation and plastic collapse as failure mechanisms. The basis for calculations is the largest crack depth obtained from non-destructive examination, briefly described in the following section. Limit loads are determined for different defect sizes and locations, and the dependence on defect (crack) length and depth is established. Integrity assessment is performed through application of Failure Assessment Diagrams (FAD).

#### PIPELINE AND MATERIAL DATA

The length of the entire pipeline at the power plant is 2030 m. The diameter is variable along the pipeline, from

#### Ključne reči

- cevovod
- ocena integriteta
- metoda konačnih elemenata
- FAD dijagram

#### Izvod

Tema ovog rada je procena integriteta deonice cevovoda u hidroelektrani Pirot. Veličina oštećenja oblika prsline, najveća dubina, određena je na osnovu rezultata ispitivanja bez razaranja - najveća dubina je usvojena kao početna vrednost pri proceni nosivosti. Takođe, dimenzije prsline (dužina i dubina) su varirane. Granične vrednosti pritiska su određene primenom 3D i 2D modela cevi sa uzdužnim prslinama na spoljašnjoj površini. Takođe, ispitan je uticaj zatezanja na nosivost cevi sa obimnim prslinama. Integritet cevovoda sa oba tipa prsline (uzdužnim i obimnim) je ocenjen primenom FAD dijagrama.

Ø 3000 mm to Ø 3500 mm. The maximum pressure in the pipeline is 2.5 MPa, and the pressure in the analysed section is 1.26 MPa. Nominal pipe wall thickness is 22 mm. The pipeline material is S275J2G3, /10/. Chemical composition and tensile properties are shown in Tables 1 and 2.

Table 1. Chemical composition (wt. %), /10/.

Material	C	Si	Mn	Cu	S	P
S275J2G3	0.210	-	1.60	0.060	0.035	0.045

Table 2. Tensile properties, /10/.

Material	Yield stress (MPa)	Ultimate tensile strength (MPa)	Elongation at fracture (%)	Impact energy (J/cm <sup>2</sup> )
S275J2G3	min. 265	430 - 560	21 - 23	27 (-20 °C)

Experimental examination of the pipeline included the following non-destructive methods: visual examination, magnetic particles, penetrants, ultrasound, radiography, as well as metallography through replica testing. Details can be found in /11/, while some aspects related to this work are mentioned in the remainder of this section.

Non-destructive testing is performed mainly in the zones of welded joints, as shown schematically in Fig. 1. On this part of the pipeline, according to the design documentation, the vertical slope is about 7 degrees, while the horizontal slope is about 10 degrees. The diameter of the pipe changes

from  $\varnothing$  3500 mm to  $\varnothing$  3340 mm (the remainder of the pipeline contains segments of smaller diameter, but not below  $\varnothing$  3000 mm).

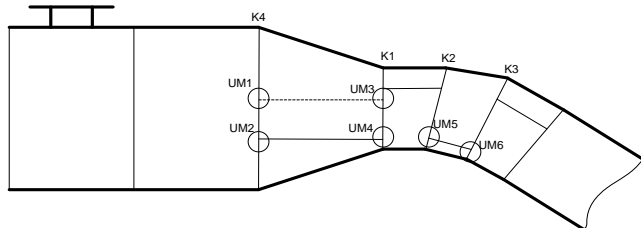


Figure 1. Examined pipe section, /11/.

Visual examination of welded joints in the analysed pipeline segments has revealed some cracks on the external surface in the weld metal, base metal and heat affected zone. On the internal surface, the cracks are observed in the base metal. The largest crack depth is 2.5 mm, while the largest length is 540 mm.

Examination by application of magnetic particles and penetrants has revealed some cracks on both external and internal surfaces of the pipeline. An example of the result of magnetic particle testing is shown in Fig. 2.



Figure 2. Cracks in base metal observed by magnetic particles, /11/.

Ultrasonic testing is also applied; one of the aims is to further inspect the severity of defects. In the base metal, crack depths ranging from 1.5 to 2.5 mm are observed, while more severe defects are found in the weld metal - depths from 3.5 to 10 mm, /11/ (note: crack depth  $a = 10$  mm represents almost half of the nominal wall thickness  $t = 22$  mm). These data are the starting point for integrity assessment which is presented in this work. The load carrying capacity of the pipeline is analysed in the presence of an initial crack of depth equal to half of the wall thickness ( $a/t = 0.5$ ).

Metallographic tests by replicas revealed a ferrite-pearlite structure in the base metal, and coarse grain ferrite-pearlite in the weld metal, both with non-metallic inclusions and corrosion products. Also, this technique revealed some micro and macro cracks in both materials, /11/.

## INTEGRITY ASSESSMENT

### Finite element models

Determination of the parameters necessary for structural integrity assessment is performed by applying the finite element method. Software package Abaqus® is applied, and

the influence of crack-like defects on the pipeline integrity is assessed. Nominal diameter and wall thickness of the pipe are 3340 mm and 22 mm, respectively.

In accordance with the principles of structural integrity assessment, the analysis is conservative; initial depths of cracks are adopted based on maximum values at any point. Therefore, the depth of both axial and circumferential cracks considered in the models are  $a/t = 0.5$ . This ratio is varied in order to determine its influence on the load carrying capacity, while crack length is also varied.

### Pipe with axial surface crack exposed to pressure loads

A three-dimensional model of the pipe with a surface axial crack is formed by application of quarter-symmetry, Fig. 3. Of course, the internal pressure is defined on the entire internal surface of the pipe, while appropriate symmetry boundary conditions are introduced at symmetry planes. There are no issues with pressure loads on crack faces since the crack is on the external surface.

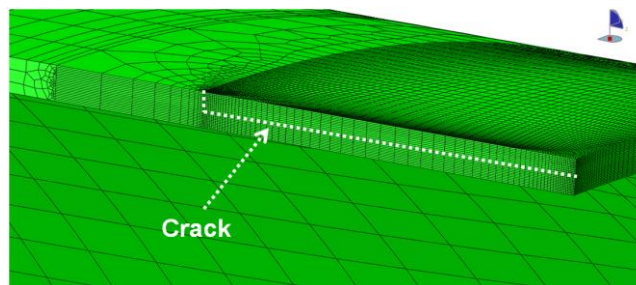


Figure 3. Finite element model of the pipe with axial surface crack.

The model shown in Fig. 3 is one of analysed 3D models; various crack depths ( $a$ ) and half-lengths ( $c$ ) are also considered. However, the axial crack is also modelled by 2D model, Fig. 4. Such a situation corresponds to infinite crack length, i.e. to the most severe defect with considered depth, that gives the lower bound of the load carrying capacity for a structure with crack. These models are analysed in plane strain conditions because the pipeline segment length is the dimension normal to the FE model plane.

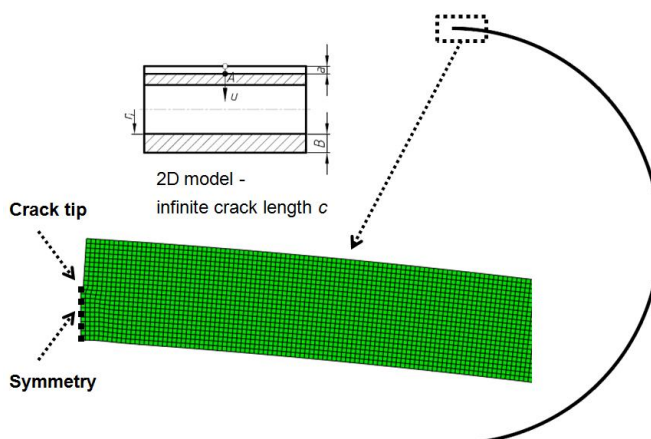


Figure 4. Simplified 2D model (plane strain, corresponding to infinite crack length).

Finite element meshes are formed by using hexahedral elements (in 3D) and quadrilateral elements (in 2D). These finite elements in Abaqus software are denoted as C3D20R

and CPE8R. Both elements have reduced integration order (shown by letter 'R'). In the 2D model, the formulation is plane strain. The properties of the base material are used in calculations. Limit load is the loading level which leads to failure of the structure due to excessive plastic deformation of the ligament ahead of the crack front. Limit loads for all pipeline configurations considered here are determined from FE models with elastic-perfectly plastic material behaviour. This approach is in accordance with many studies from literature, such as /3, 4/. In order to avoid convergence problems, the RIKS option in Abaqus is applied. Limit load values are obtained by applying the LPF factor (Load Proportionality Factor), /12/.

Dependence of limit pressure on the length of the axial crack is shown in Fig. 5. Results include three 3D models with different crack half-length  $c$ , and also a 2D model with infinite crack length. As mentioned previously, 2D models represent the lower bound for the considered crack depth (in Fig. 4,  $a/t = 0.5$ ). Also, the influence of the variation of crack depth on the limit load is considered, Fig. 6, using the example of 3D models with crack half-length  $c = 100$  mm and 2D models.

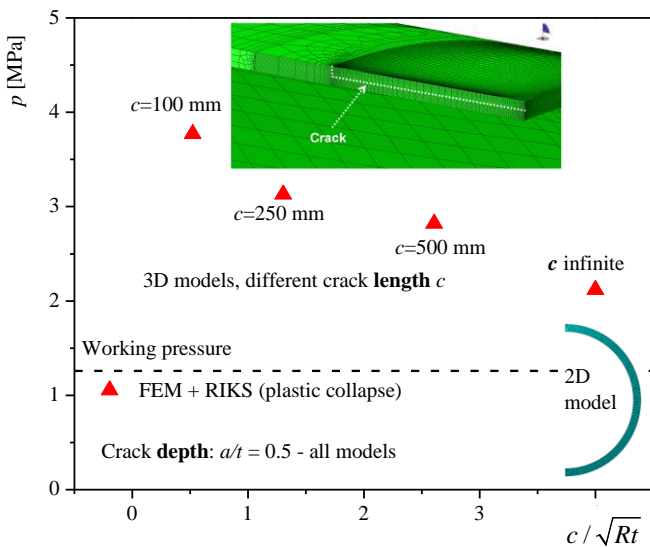


Figure 5. Limit pressure vs. length of axial surface crack.

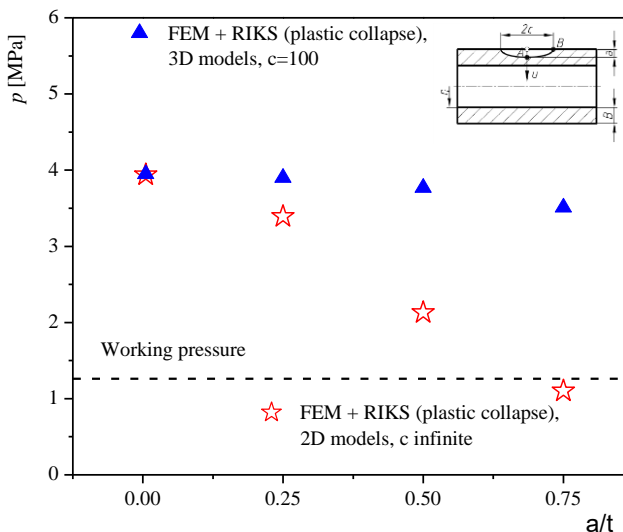


Figure 6. Limit pressure vs. crack depth.

Besides the lower load carrying capacity predicted for 2D models, it can be seen that the influence of crack depth is much more prominent.

Based on the applied conservative approach in all steps of the analysis, it can be concluded that the crack of depth equal to half of the pipe wall thickness is safe with respect to plastic collapse. This can be stated for both 3D models with finite crack length and 2D model representing the infinite crack length - obtained limit pressure is higher than working pressure. Only for the most severe analysed defect, the crack with infinite length and depth  $a/t = 0.75$ , the limit pressure is below working pressure. For finite crack length (3D model,  $c = 100$  mm), limit pressure is higher than working pressure even for this crack depth.

*Pipe with circumferential crack exposed to tensile load*

As mentioned previously, non-destructive tests revealed the existence of both axial and circumferential defects in the pipeline. One of the cracks with the largest dimensions is found in the circumferential direction. Such defects are not significantly influenced by internal pressure, but they are critical for tensile or bending loads on pipelines in exploitation. Here, the limiting (and the most conservative) case is considered, with a 360° crack along the entire circumference, as shown in Fig. 7. This figure shows the definition of the axisymmetric model and a detail of the mesh around the crack. The axisymmetric finite element CAX8R is used. Normal stresses in axial direction, such as those acting on the pipe in Fig. 7, can be a result of pipeline weight and type/position of supports. For example, such pure tensile loading is present in oil or gas rigs.

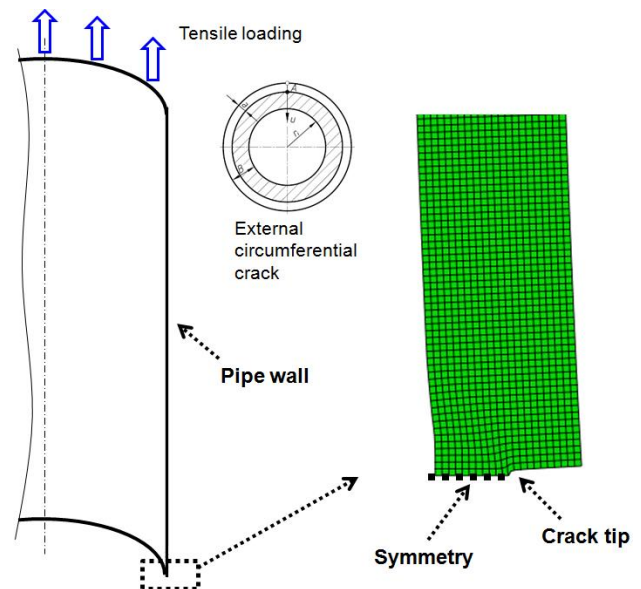


Figure 7. Axisymmetric model of pipe with circumferential crack exposed to tensile loading.

The influence of crack depth on the limit load of the pipe with a circumferential crack exposed to tensile loading is shown in Fig. 8. The values represent the distant stress in the region of the model far from the crack tip. In Fig. 8, the limit tensile stress for the crack depth equal to half of the wall thickness ( $a/t = 0.5$ ) is 160 MPa. There are no measurement data regarding tensile stress in the pipeline, so it

cannot be concluded whether the structure is endangered with respect to tensile loading. However, a comparison of obtained values with some experimental data, such as those based on strain gauges or digital image correlation (stereometric measurement) would lead to either determining the maximal load for the observed crack depth or the maximal acceptable crack depth at a given load level.

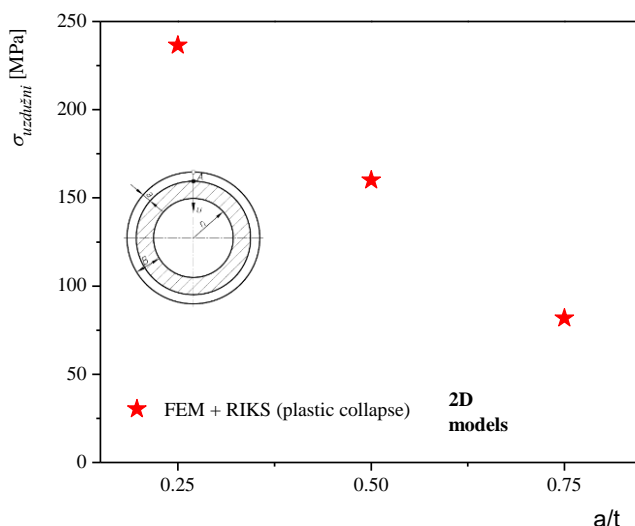


Figure 8. Limit tensile stress (corresponding to plastic collapse) vs. depth of circumferential crack.

*Integrity assessment by application of failure assessment diagram (FAD)*

Results obtained in previous figures correspond to failure prediction of cracked pipelines due to excessive plastic deformation that leads to plastic collapse. In order to assess their integrity, the other failure mechanism, fracture, also has to be taken into account. The work pressure  $p = 1.26$  MPa is used for assessment, i.e. the influence of cracks of different dimensions on the working pressure is determined. Values of stress intensity factors are determined from the numerical model using the domain integral method in Abaqus, /12/.

The calculation is based on SINTAP/FITNET procedure, level 1, /13, 14/. In the failure assessment diagram, the following quantities are given for the case of the pipeline exposed to internal pressure loads:

$$L_r = \frac{p}{p_Y},$$

$$K_r = \frac{K}{K_{mat}}.$$

In this expression,  $p$  is the working pressure in the considered pipeline segment ( $p = 1.26$  MPa), and  $K$  is the stress intensity factor. For determining the position of point ( $L_r, K_r$ ) on the FAD diagram, the limiting values of these quantities must be determined for the considered structure, material properties, and crack geometry.

The limit pressure  $p_Y$  is actually obtained in previous sections for different crack dimensions. Since the fracture toughness value,  $K_{mat}$  or  $K_{Ic}$ , is not available for the particular pipeline, it is determined based on impact energy, /15/:

$$K_{mat} = (12\sqrt{C_V} - 20)(25/t)^{0.25},$$

where:  $C_V$  is impact energy; and  $t$  is pipe wall thickness. The obtained value is:  $K_{mat} = 1383$  MPa√mm.

The expressions for the limit FAD curve are, /13, 14/:

$$f(L_r) = (1 + 0.5L_r^2)^{-1/2} \quad \text{for } 0 \leq L_r \leq 1,$$

$$f(1) = (\lambda + \frac{1}{2\lambda})^{-1/2},$$

$$f(L_r) = f(1)L_r^{(N-1)/2N} \quad \text{for } 1 \leq L_r \leq L_r^{max},$$

$$\lambda = 1 + \frac{0.0375E}{\sigma_Y} \left(1 - \frac{\sigma_Y}{1000}\right),$$

$$N = 0.3(1 - \sigma_Y/\sigma_m),$$

$$L_r^{max} = 0.5(1 + \sigma_m/\sigma_e).$$

In these equations,  $\sigma_Y$  and  $\sigma_m$  are the yield and tensile strength of the material, while  $N$  is the hardening exponent.

In Fig. 9, integrity assessment is shown for different crack depths, where the most conservative case is considered – 2D models that represent the infinite crack length. It can be seen that, under all above-mentioned conditions, the crack depth of 50% of pipe wall thickness leads to the point in the potentially unsafe region of the FAD diagram. Two other cracks with smaller depths are within the safe region. Also, it can be seen that the influence of fracture, as a failure mechanism, is more pronounced in comparison with plastic collapse. For example, the crack depth  $a/t = 0.5$  leads to  $K_r > 1$ , while  $L_r$  is around 0.6.

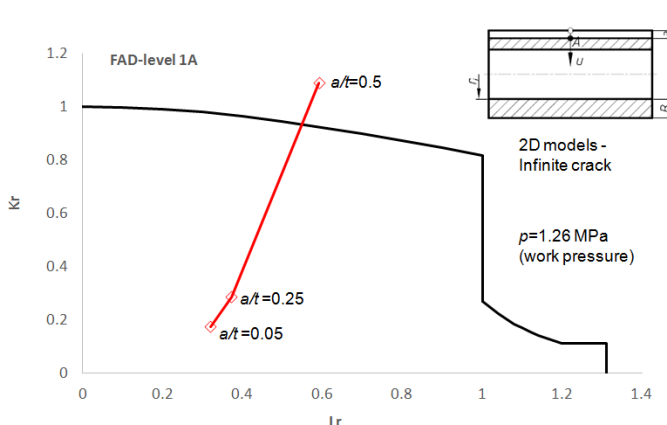


Figure 9. FAD diagram with various axial crack depths (2D model - infinite crack length).

The influence of circumferential crack on the integrity of the pipeline under tensile loading is shown in Fig. 10. The considered tensile stress values are 120, 90 and 60 MPa. Due to different loading conditions in comparison with the previous FAD diagram, it should be noted that  $L_r$  value is determined from stress values:

$$L_r = \frac{\sigma}{\sigma_Y}.$$

If tensile stress values for the pipeline are available (e.g. determined from strain gauges or digital image correlation, that can be used for the stress calculation for elastic deformation), the diagram in Fig. 10 can be used for integrity

assessment of a particular pipe segment under exploitation conditions.

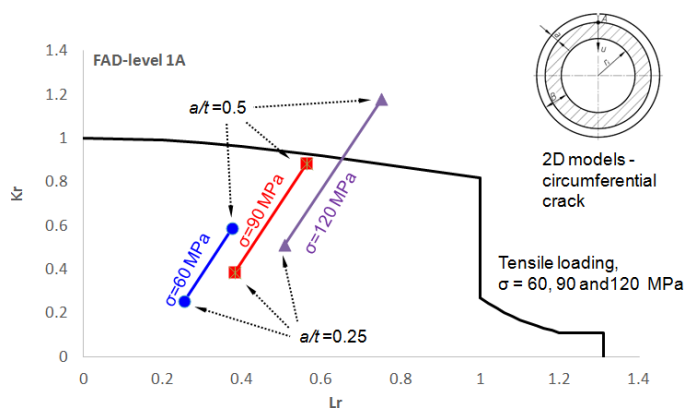


Figure 10. FAD diagram - various tensile stress values and circumferential crack depths (2D model - tensile loading).

## CONCLUSION

In this work, limit loads are determined for various configurations of defects (cracks) in a pipeline section from the hydropower plant Pirot. Finite element method is used for determining limit loads and fracture mechanics parameters (stress intensity factors). Integrity assessment is performed in accordance with SINTAP/ FITNET procedure.

Axial surface cracks of various depth and length are considered, and the largest depth observed experimentally does not pose a threat to the integrity of the pipeline, regardless of crack length. However, when fracture initiation is also considered in the failure assessment diagram, it turns out that this crack depth is in the potentially unsafe region for the most severe case – the infinite crack length. For circumferential cracks, the influence of tensile loading on the limit loads and integrity is also determined since this loading direction is critical in this particular case.

## ACKNOWLEDGEMENTS

This work was supported by the Ministry of Education, Science and Technological Development of the Republic of Serbia (Contracts No. 451-03-68/2020-14/200135, 451-03-68/2020-14/200012).

## REFERENCES

1. Dutta, B.K., Saini, S., Arora, N. (2005), *Application of a modified damage potential to predict ductile crack initiation in welded pipes*, Int. J. Pres. Ves. Piping, 82(11): 833-839. doi: 10.1016/j.ijpvp.2005.07.001

2. Gubelj, N., Vojvodić Tuma, J., Šuštaršić, B., et al. (2007), *Assessment of the load-bearing capacity of a primary pipeline*, Eng. Fract. Mech. 74(6): 995-1005. doi: 10.1016/j.engfracmech.2006.08.013
3. Kim, Y.-J., Shim, D.-J., Huh, N.-S., Kim, Y.-J. (2002), *Plastic limit pressures for cracked pipes using finite element limit analyses*, Int. J. Press. Ves. Piping, 79(5): 321-330. doi: 10.1016/S0308-0161(02)00031-5
4. Huh, N.-S., Kim, Y.-J., Kim, Y.-J. (2007), *Limit load solutions for pipes with through-wall crack under single and combined loading based on finite element analyses*, J. Pres. Ves. Technol. – Trans. ASME, 129(3): 468-473. doi: 10.1115/1.2748828
5. Arafah, D., Madia, M., Zerbst, U., et al. (2015), *Instability analysis of pressurized pipes with longitudinal surface cracks*, Int. J. Pres. Ves. Piping, 126-127: 48-57. doi: 10.1016/j.ijpvp.2015.01.001
6. Chiodo, M.S.G., Ruggieri, C. (2009), *Failure assessments of corroded pipelines with axial defects using stress-based criteria: Numerical studies and verification analyses*, Int. J. Pressure Ves. Piping, 86(2-3): 164-176. doi: 10.1016/j.ijpvp.2008.11.011
7. Medjo, B., Rakin, M., Arsić, M., et al. (2012), *Determination of the load carrying capacity of damaged pipes using local approach to fracture*, Materials Trans. - JIM (Japan Institute of Metals and Materials), 53(01): 185-190.
8. Milovanović, A., Sedmak, A. (2018), *Integrity assessment of turbine flat cover pipe*, Struc. Integ. and Life, 18(3): 181-183.
9. Amara, M., Bouledroua, O., Hadj Meliani, M., et al. (2018), *Assessment of pipe for CO<sub>2</sub> transportation using a constraint modified CTOD failure assessment diagram*, Struc. Integ. and Life, 18(2): 149-153.
10. SRPS EN 10025-1, Hot rolled products of structural steels - Part 1: General technical delivery conditions, Institute for Standardization of Serbia, 2011.
11. Arsić, M., Grabulov, V., Mladenović, M., Savić, Z. (2018), *Analysis of current state and strength evaluation of the pipeline at hydro power plant 'Pirot' (in Serbian)*, Zavarivanje i zavarene konstrukcije, 63(1): 17-22.
12. Abaqus Analysis User's Guide, Dassault Systèmes Simulia Corp., 2018.
13. SINTAP: Structural Integrity Assessment Procedure - Final Report EU project BE95-462 (1999).
14. FITNET: European Fitness-for-Service Network, <http://www.eurofitnet.org>
15. Zerbst, U., Schödel, M., Webster, S., Ainsworth, R., Fitness-for-Service Fracture Assessment of Structures Containing Cracks (A Workbook based on the European SINTAP/FITNET procedure), Academic Press, 2007, p.320.

© 2020 The Author. Structural Integrity and Life, Published by DIVK (The Society for Structural Integrity and Life 'Prof. Dr Stojan Sedmak') (<http://divk.inovacionicentar.rs/ivk/home.html>). This is an open access article distributed under the terms and conditions of the [Creative Commons Attribution-NonCommercial-NoDerivatives 4.0 International License](https://creativecommons.org/licenses/by-nc-nd/4.0/)